EXPERIMENTAL AND NUMERICAL ANALYSIS OF LASER REFLECTION FOR OPTICAL-THERMAL PROCESS MODELING OF TAPE WINDING

Amin Zaami[1,2], Ismet Baran[1,3], Remko Akkerman[1,4]

[1]Faculty of Engineering Technology, Chair of Production Technology, University of Twente, The Netherlands
[2]Email: a.zaami@utwente.nl
[3]Email: i.baran@utwente.nl
[4]Email: r.akkerman@utwente.nl

Keywords: Laser assisted tape winding, optical-thermal model, thermoplastic tape, composites.

ABSTRACT

Temperature measurement in laser assisted tape winding (LATW) has been a source of great interest since the laser winding process becomes a popular way for producing new thermoplastic products. The accurate temperature of tape surfaces in this process is highly dependent on the optical behavior of materials. Changing the texture of materials is expected during the process which consequently causes changing in reflectance from the surfaces. The reflectance measurement is considered in the category of the optical measurement. In this research, the reflectance measurement is studied to characterize the optical response of material surface in a high temperature up to the melting point of the materials by using a heating plate. To do so, different thermoplastic materials were employed for capturing reflection patterns. It was found that different shapes and intensities can be attained for a specific material. Furthermore, during increasing the temperature, some shrinking in width of the tape has been observed probably due to relaxation of the residual stresses which also has an influence on texture architecture of the tape by moving fibers on the surface and changing the distance between them. The current observations suggest new modifications for the already developed BRDF function [1] to simulate the anisotropic reflection behavior as a function of temperature and surface texture. A three-dimensional (3D) optical model is used to simulate the laser intensity distribution on the tape surface. The predicted heat flux distribution is used in a 2D steady-state fully implicit thermal model considering advection term in the heat transfer equation to calculate the temperature distribution. Moreover, this gives us a better understanding of the phenomenological interaction on the surface of different samples at different temperatures to predict the surface temperature of the tape and substrate more accurately based on the proposed process models.

1 INTRODUCTION

Laser assisted tape winding (LATW) is a technique used to create a product with continuous fiber reinforced (thermo) plastic (FRP) unidirectional (UD) tapes. The traditional manufacturing of composites which often involves thermosetting resins is slow, labor intensive and has to be post-processed. The LATW can get the cycle times down and there is potentially no post processing necessary. In general, setting up the production of a new part might take a considerable amount of time to find the optimum process parameters for enhanced product properties. In order to eliminate the expensive trial-and-error based design approaches for process and product design, the development of a physics-based process simulation tool is essential.

Fig. 1 shows schematically a LATW process. One of the important aspects of the LATW process is the fusion bonding during the consolidation of tapes by the roller as depicted in Fig. 1. This process is described as applying heat and pressure to the thermoplastic tape. The steps that are taken are thermal softening of the material, intimate contact, healing and ends with a bonded material. Softening is a result of heating the surface of the tape and laminate with a laser source. The compaction roller exerts the pressure to consolidate incoming tape and laminate. The contact area that connects the two surfaces is called the intimate contact. The temperature and pressure at the interface lead to interdiffusion of

polymer chains on the contact area, which can be defined as healing. The consolidation roller also cools down the tape as well as the interface at which the bonding occurs. Based on the main bonding mechanisms described above, the thermal history of the interface is considered to be a key parameter [1-4].

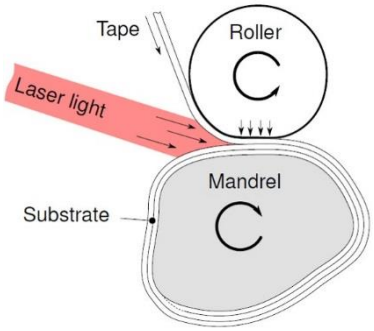

Figure 1. Schematically drawing of LATW process.

The bonding strength of the final product is heavily dependent on the temperature history of the tape and the laminate. When the temperature of the thermoplastic resin is not high enough the intimate contact areas get very small and this results in a poor bonding. On the other hand, too much heat might degrade the resin material. [1]. Therefore, the temperature control during the LATW process is crucial for product quality. The accurate temperature prediction of tape surfaces in this process is highly dependent on the optical behavior of the texture of materials [5].

Regarding the experimental and the numerical modeling, several studies have been carried out to simulate the LATW or laser assisted tape placement (LATP) processes. The focus here is on the studies considering coupled optical and thermal models [1, 2, 6]. The temperature prediction for the LATP was developed in [2] where a ray-tracing method together with a one-dimensional (1D) thermal model was used. Another study was performed by Stokes-Griffin [6] who developed a more detailed model for the LATP. The optical model used reflection in 3D together with a 2D thermal model implemented in ANSYS. The composite surface was modeled as a collection of micro-half-cylinders. Both aforementioned optical models dealt with flat substrates. However, when a cylindrical substrate is used with different geometrical orientations (oblique angle), a more complicated optical-thermal process model should be taken into account since the geometry complexity can play an important role on the energy absorption/reflection and subsequently temperature distribution. In this regard, another study was carried out in [5] to simulate the effect of non-specular reflection model. However, the effect of changing surface texture during the process on the nip-point temperature is still unknown. In addition, there is a lack of a general optical model that considers the effects of an oblique angle and winding direction in the literature.

In this paper, an experiment regarding the reflection pattern at the melting temperature has been reported. Then, the simulation for complex setup configurations of a LATW process is performed. The main goal is to have an accurate model for inline monitoring and quality assurance which is a part of EU funded ambliFibre project. The final optical-thermal model should be able to compensate the difference between the predicted and the measured values of the nip-point to have a better product properties with minimized energy consumption. To reach that goal, certain assumptions in an efficient computational algorithm for the LATW process is implemented. Ultimately, the suggestion for considering non-specular model considering which is temperature dependent will be proposed.

2 MATERIALS AND METHODS

In LATW process, the temperature at the nip point is not constant with a specific setup configuration for different thermoplastic materials. The laser light strikes the tape, then the majority of the laser beams is absorbed and some portion is reflected (it is assumed that no laser ray passes the tape). The absorbed part of the energy results in heating the material. The reflection of a thermoplastic UD tape is dependent on the process setup such as the angle of incident and material status as a function the temperature. Based on the resin and the fiber content of the material as well as the material temperature and

orientation, the reflectance of the incoming laser ray can be different. This is where the need of an accurate model comes into account for the optical tape properties. Thus, the objective is to create an optical model considering material texture effect in combination with a thermal model of a composite surface activated by a laser. To get insight in the reflection of the laser and the change of reflection due to molten resin, reflection experiments were designed.

In the reflection experiments at elevated temperatures, three materials were tested. Those materials were PA6/GF, PA12/CF and PVDF/CF where GF stands for glass fiber and CF is the carbon fiber. To investigate the difference between the reflection pattern of solid and melted thermoplastic material, pictures of the reflections were taken at the room temperature and at the melting temperature. With those pictures, a discussion can be started over the visual and the measured differences the reflection behavior. The experimental setup is shown in Fig. 2.

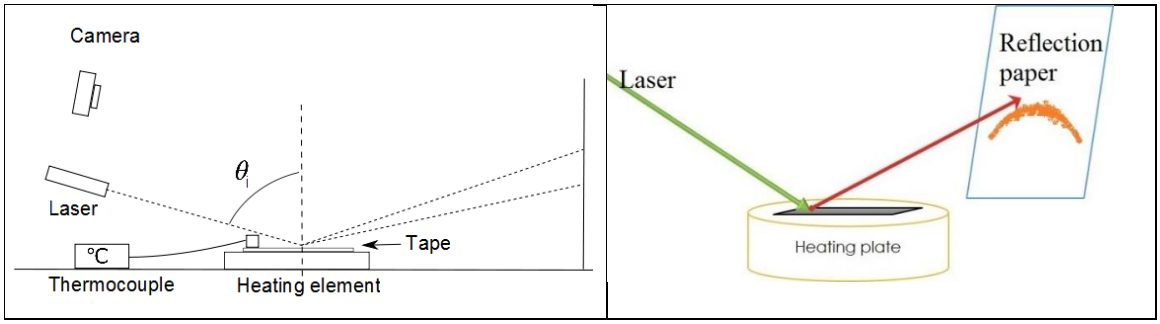

Figure 2. The heating plate setup.

PA6/GF is standing for polyamide with glass fibers. PA12/CF is a polyamide with carbon fibers. The melting temperature of PA6/GF (220º) is 40º higher than PA12/CF (178º). PVDF/CF is a polyvinylinee fluoride with carbon fibers. In Table 1 different material properties are stated. The difference in fibers will be a major concern when looking at the reflection. Calculating the reflectance at θ_i= 70º, the reflection of the glass fiber is 0.17 and the carbon fibers 0.28 on a scale of 0 to 1. Because the adsorption coefficient of glass fiber is very low (and the transmittance very high), black pigment (often carbon black) is added to the resin of laser processed glass fiber composites.

The setup that was used to test the scatter of the different tapes is described in this section. The setup representation is seen in Fig. 3. The following equipment was used to conduct the experiment: Tapes, pieces of 50 mm of PA6/GF, PA12/CF and PVDF/CF, Uniphase laser model 1103p with a beam diameter of 0.63mm and wavelength of 632 nm. The heating element was an IKA RET basic with an ETS-D5 thermometer to control the temperature of the heating plate. Other tools have been stated hereunder:

- Nikon D5000 reflex camera with an AF-S DX VR
- Zoom-NIKKOR 18-200mm f/3.5-5.6G IF-ED lens.
- Rigid stand for the camera.
- Rigid stand for the laser.
- RS Heat Sink Compound, 0.65 W/m.K.
- Fluke 561 IR thermometer with a thermocouple

Different components were fixed in a position to minimize the variation in the obtained results. The thermocouple was fixed on the tape to measure the real temperature. The camera has a fixed position, so all the pictures were from the same angle and distance. The laser was put under an angle of incident which was 70º .as aforementioned. The fiber orientation angle with respect to the laser beam was set to 0º. The tapes were placed on the heating plate with a dot of the RS Heat Sink Compound to maximize the heat transfer.

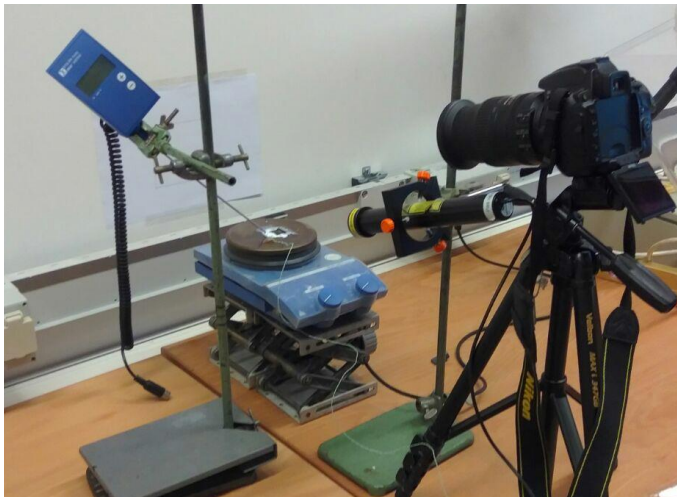

Figure 3. Reflection measurement setup.

Table 1. Properties of the used materials.

Material	Tape width (mm)	Thickness (mm)	Fiber volume(%)	Melting point (°C)	Glass transition temperature(°C)	Refractive index	Crystalinity
PA6/GF	25	0.26	60	220	60	1.49	Semi-crystalline
PA12/CF	20	0.4	50	178	40	2.45	Semi-crystalline
PVDF/CF	26.5	0.25	45	177	-30	2.45	Semi-crystalline

In Fig. 4, it can be seen that reflection of PA12/CF did not visually change when the temperature goes over the melting point. The reflection pattern of PA6/GF was changed substantially when the resin started to melt, see Fig. 5. PVDF/CF also had almost no visual changes between the melted and solid phase of the resin as seen in Fig. 6. An explanation can be found in [5] where it was stated that the resin (PEEK) had a small effect on the scatter and the dominant scattering mechanism was the carbon fibers. It can be inspired that this can also be the case here. Even when the resin is molten the reflection is not changed. On the other hand, for the experiment with PA6/GF, this is not the case. The black pigment in the resin causes the resin having the dominant scattering mechanism. Fig. 5 resembles the scattering of a fiber dominant mechanism can be explained by a small layer of resin that covers the glass fiber. When transforming into a melted state it is clearly seen that the scatter pattern is continually changing. The surface tension of the resin shapes the geometry of the tape and tries to get into the least energetic state which results in different reflection patterns. For PVDF/CF, the reflection behavior is similar to PA12/CF. It is worth to mention that the reflection pattern gets sharper which means fibers become more dominant scattering mechanism than at the room temperature. Accordingly, the surface texture was investigated under an optical microscope. The microscopic images for the intact and heated surface of PA6/GF are shown in Fig.7. Some sort of inclusions can clearly be seen on the surface of the heated sample for PA6/GF probably due to the deconsolidation at melt temperature. The surface is also not glassy at melt temperature as compared with the intact sample at room temperature.

Figure 4. Reflection at the room (left) and the melting temperature (right) of PA12/CF.

Figure 5. Reflection at the room (left) and the melting temperature (right) of PA6/GF.

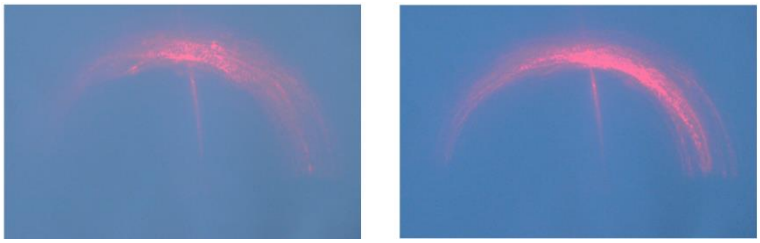

Figure 6. Reflection at the room (left) and the melting temperature (right) of PVDF/CF.

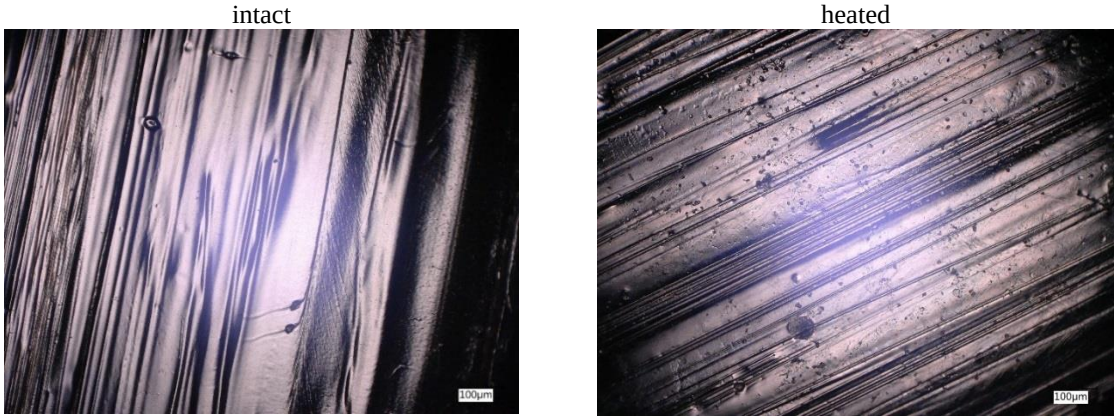

Figure 7. Microscopic image of PA6/GF surface before (left) and after heating (right).

The heated samples of PVDF/CF and PA6/GF are shown in Fig. 8 for comparison purpose. The difference in the surface texture is clearly seen. The fibers are the reason for the arc-shaped reflection for the PVDF/CF. This arc-shaped is not seen for the heated sample of the PA6/GF. However, the reflection of PVDF/CF heated sample is still dominated by fibers. Thus, it can be concluded the configuration of the fibers is changed for PA6/GF after heating and this indicates that the fiber movement is the dominant mechanism for the reflection behavior.

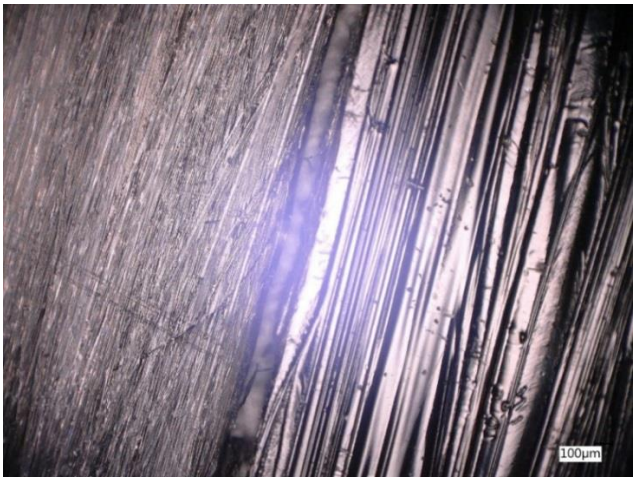

Figure 8. Microscopic image of PVDF/CF (left) and PA6/GF (right) after the heating experiment.

3 PROCESS SIMULATION

The optical-thermal process model has been developed in Matlab. The optical part calculates the laser intensity distribution based on a 3D ray-tracing model, and the thermal model which is coupled with the optical model predicts the temperature distribution on the tape and substrate surfaces. There is also an interface function which links these two computational parts, i.e. optical and thermal, and entering parameters for the computational part as well as the illustration of the results. Five different objects were implemented into the optical model, and the geometrical parameters were defined which can be easily controlled by the user to produce different geometries and process conditions including winding speed. Because of the complexity of different material reflection based on the manufacture, quality, and some other unknown parameters which influence the reflectance and energy absorption, here the analysis will be performed for the specular case to see the effect of complex orientation of the laser and incoming tape. Furthermore, the effect of roller deformation is not considered in the simulations. The nip-point temperature is the point of interest in this study since the nip point temperature directly affects the bonding of the tape.

3.1 Optical model

Regarding the optical model, the ray-tracing approach has been employed. In this method, calculation of reflection for each ray will be performed separately. The intersection points will be calculated and the reflection ray will be drawn. All these computations will be executed based on the exact mathematical relations without any simplification to prevent any misplacements of the input energy. The schematic of this has been shown in Fig. 9.

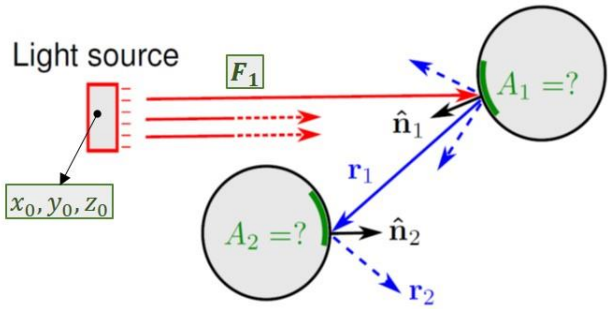

Figure 9. Ray tracing as applied to the LATW process.

The intersection between a ray and an object can be described by EQ.(1). The equation of the 3D line ($F1$) is:

$$\frac{x-x_0}{a_1}=\frac{y-y_0}{b_1}=\frac{z-z_0}{c_1}=F_1 \quad (1)$$

Where a_1, b_1, c_1 are the laser direction, and x_0, y_0, z_0 are the laser position. The equation of the 3D arbitrary surface ($F2$):

$$a_2 x\vec{i} + b_2 y\vec{j} + ((c_2 x) + (d_2 y))\vec{k} = A_1 \quad (2)$$

The coefficients a_2, b_2, c_2, d_2 of A_1 in EQ.(2) can be non-constant (like $a_2 = a_2(x, y)$). Thus, equating these two equations (F_1) and (A_1), it is possible to find the intersection(s) of two 3D objects, if there is an intersection.

$$A_1(x_{int}, y_{int}, z_{int}) = F_1(x_{int}, y_{int}, z_{int}) \quad (3)$$

However, since there are 4 effective objects (tape, substrate, roller, and mandrel) in the LATW process which influence the optical behavior on the tape and substrate, there should be a smart algorithm for decision making to figure out which object has the actual intersection with the laser and reflection rays (The further explanation of this algorithm is not explained here). Thus in the optical model, the intensity on the surfaces is obtained. The intensity for each location is then transferred to the thermal domain as a heat source. The illustration of the optical model results is depicted in Fig. 10.

Side view: Front view:

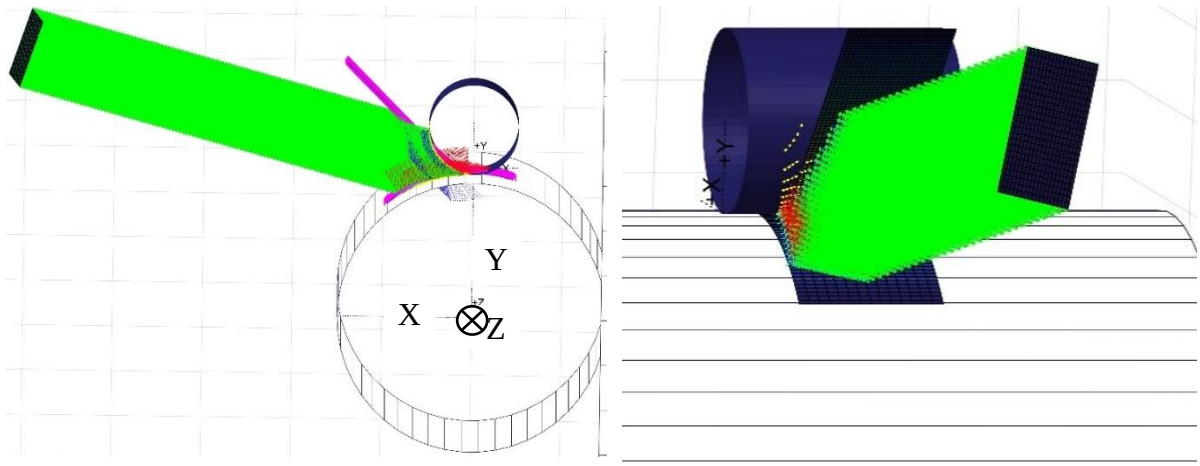

Figure 10. 3D optical model including Laser (green lines), cylinders (Roller and mandrel), tape and substrate (purple color).

Three cases were studied here regarding the laser location and orientation. The different laser configuration together with winding direction setup is shown in Table 2 and Fig. 11. L_xyz0 is the center of the laser (rectangular shape in Fig.10), and Rx, Ry, Rz are laser position with respect to the coordinate system.

Table 2. Different laser configuration parameter.

	Case1(22.5° oblique angle)	Case2 (hoop winding (zero oblique angle)	Case 3 (degrees winding angle direction)
Ray in x-direction	Rx=-0.8239;	Rx=-0.8239;	Rx=-0.8239;
Ray in y-direction	Ry= -0.1972;	Ry= -0.1972;	Ry= -0.1972;
Ray in z-direction	Rz= -0.3455;	Rz= 0;	Rz= 0;
Laser center	L_xyz0=[50 27 35];	L_xyz0=[50 24 20];	L_xyz0=[50 24 20];
Winding angle	0°	0°	22.5°

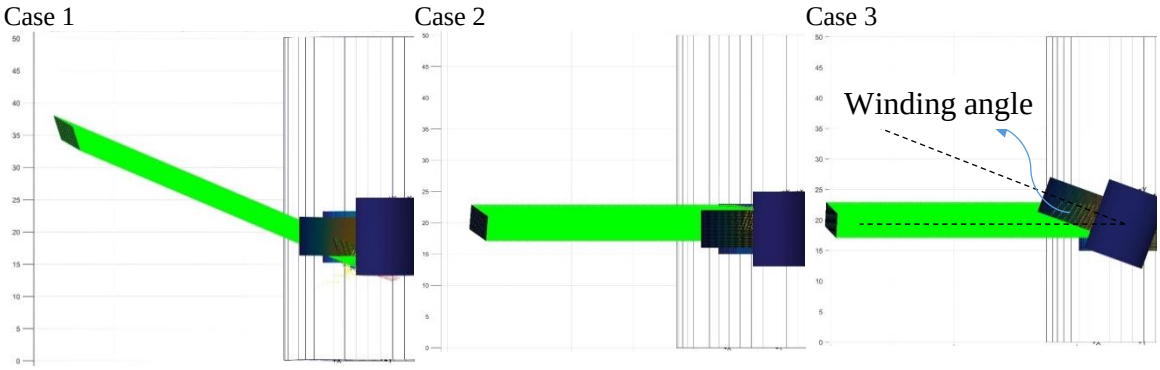

Figure 11. Different configurations of the optical model.

3.2 Thermal model

The thermal model calculates temperature based on the 2D computational model on a 3D surface geometry using the finite element method developed in Matlab as an inhouse simulation code. The actual energy distribution is received from the 3D optical model. The process is physically transient because of the presence of the velocity which plays an important role in the process. However, it might be advantageous to discard the transient terms in the heat transfer equation to acquire better computational time. Therefore, by changing the framework into the Eulerian description, the problem can be seen as a control volume case, i.e. stationary mesh in the simulation. Then, it is possible to involve velocity into the governing equation as an advection term. Thus, this model employs a steady-state diffusion equation considering advection term which is represented in EQ.(4).

$$v\frac{\partial T}{\partial x} = \alpha\left(\frac{\partial^2 T}{\partial x^2} + \frac{\partial^2 T}{\partial y^2}\right) \tag{4}$$

In this equation v is the velocity, α is the thermal diffusivity, x and y represent spatial location, and T is the temperature. Presence of the velocity term in this equation makes the PDE (partial differential equation) to become hyperbolic which is unstable if the effect of velocity would be dominant. Using some techniques in the category of the upwind method can resolve this issues in the numerical models ([7-12]). In FEM thermal model, the implicit SUPG (Streamline Upwind Petrov-Galerkin) method was implemented to obtain results in only one computational step. There were 2700 elements were used in the simulations for the tape and substrate. Regarding the domains and boundary conditions, the laser energy considered as heat sources on the surfaces of the body. Fig. 12 provides an overview of the computational domains and boundary conditions. The domain includes:

- Heat source on the nodes from the optical model
- Initial temperature 20^{o} on the left side where the material enters the domain.
- Other boundaries are adiabatic

The thermal properties of the tape were taken from [5]. The winding speed in the simulations was 150 mm/s. The calculation domain was 20x60 mm.

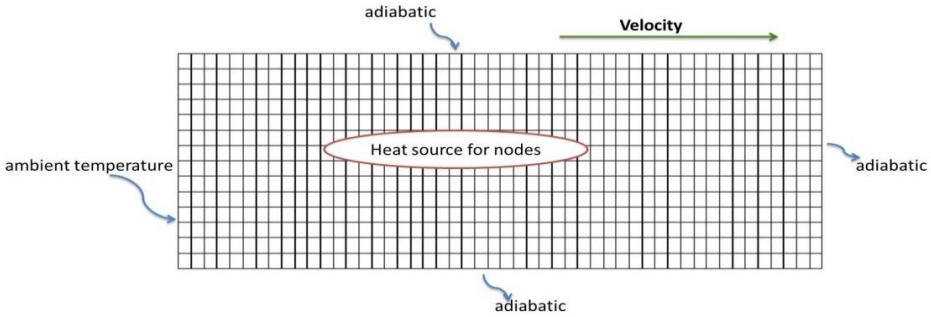

Figure 12. Boundary conditions of the tape surface.

4 RESULTS AND DISCUSSION

The Gaussian distribution based laser intensity ($\exp(-(x^2+y^2))$) is employed in the optical model which then calculates the corresponding heat flux distribution for the thermal model. Based on the estimated heat flux distribution, the temperature distribution is calculated in a 2D thermal model. The results are illustrated in Fig. 13. Here, the focus is on the potential for modeling the different process configuration. For the case of oblique angle (case 1), most of the reflection do not have intersection with the tape, thus less temperature value is obtained. The temperature distribution can be investigated along the width of the nip-point line (when tape and substrate contact each other). Temperature along the nip-point line is shown in Fig. 14. Since there is an oblique angle in case 1, it is seen higher temperature at the left side for both tape and substrate. In case 2, because the position of the laser is not exactly at the center, it makes non-symmetric temperature profile which makes higher temperature at the right side. The temperature profile of the case 3 is also not changing very much comparing to case 2 (less than 30 °C). Therefore, different temperature profile trend has been captured here for the incoming tape and the substrate. It is worth to mention that, this trend is also dependent on the process velocity and the diffusion coefficient. Since the intensity distribution of the laser on the incoming tape and the substrate is somehow not simple (effect of winding direction and Gaussian distribution), non-uniform temperature profile is seen.

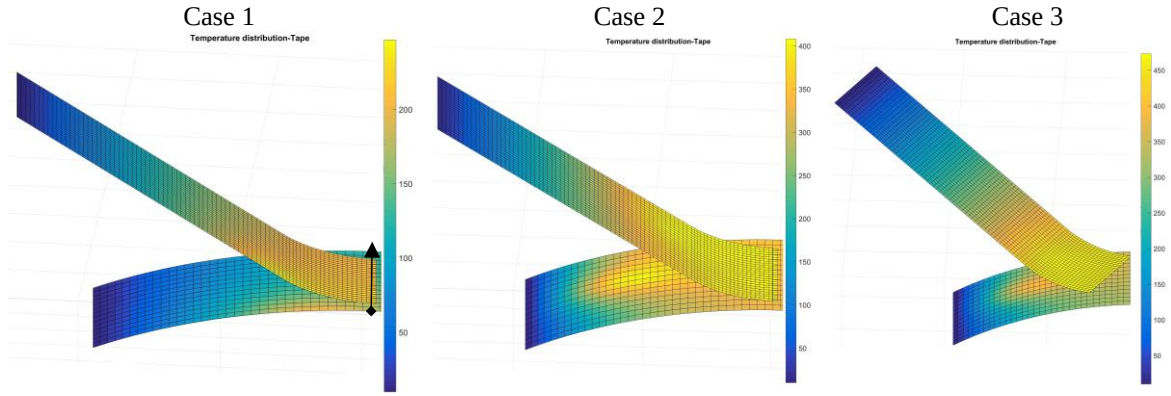

Figure 13. Temperature distribution results of tape and substrate.

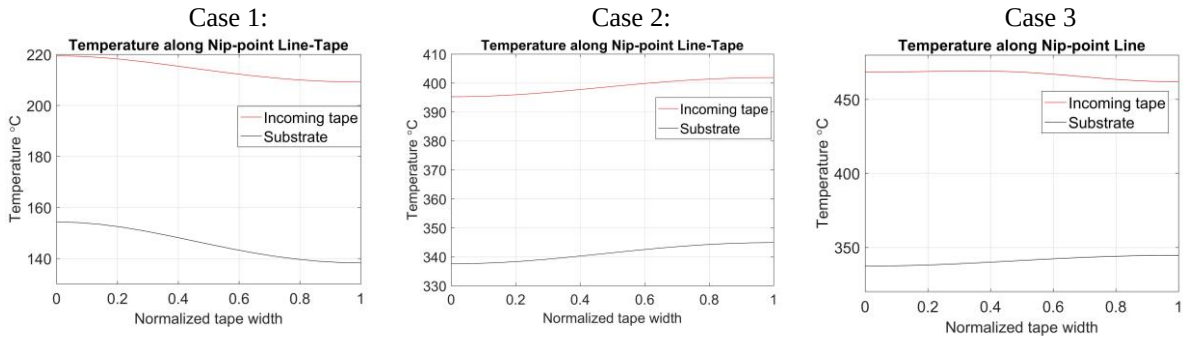

Figure 14. Temperature distribution profile along the nip-point line.

It can be concluded that the temperature profile along the width can be optimized based on the input parameters including laser setup (angle, position), optical laser distribution (uniform, Gaussian, linear). Having the optimum temperature along the nip-point is utmost crucial in order to have a good intimate contact and hence a good bonding during the consolidation. Later, the experimental results should be exploited for the simulation strategy. For carbon fiber thermoplastic tapes, there is no need to include temperature effect into the reflection model. However, for glass fiber seems necessary since reflection depends on the temperature. For capturing this effect, it is suggested to use specular reflection after melting. Nonetheless, including roughness parameters may turn the computational procedure to be complex and not suitable for in-line monitoring. The point on the tape that this transition happens, can

be captured via experimental results and this point consider as the transition point in the simulations. In [5] difference between non-specular and specular model was reported to be up to 8% of the nip-point temperature. Then, the simulation model can be able to use the experimental observation for further developments.

5 CONCLUSION

An investigation on the reflection scatter pattern of PA12/CF, PA6/GF and PVDF/CF UD tapes were conducted. The goal was to understand the reflection of thermoplastic UD tapes at elevated temperatures. It was found that the reflection is dependent not only on the angle of incident and fiber orientation but also on the temperature history. For fiber dominant scatter mechanisms the fiber orientation regarding the laser is highly anisotropic and changes with the position. For the resin dominant scattering mechanisms, the reflection changes when the resin passes its melting point. Besides, different laser distributions cause the reflection behavior of the composite to be more complicated and somewhat makes it difficult to predict the nip-point temperature for further optimization. Thus, different laser configurations can speed up the process and produce a specific temperature distribution based on the user input. The effect of oblique angle can put reflection energy on the specific area. Thus, the laser position (including oblique angle) and laser distribution are the inputs for controlling the temperature profile along the nip-point line.

Regarding the reflection model, the carbon fiber thermoplastic tapes do not need a temperature-dependent reflection model. This effect can be negligible for them. However, transition effect should be considered for the glass fiber materials.

ACKNOWLEDGEMENTS

The amblifibre project has received funding from the European Union's Horizon 2020 research and innovation program under grant agreement No 678875.

REFERENCES

[1] I. Baran, R. Akkerman, and J. Reichardt, *Optical process model for laser-assisted tape winding*, ECCM 17, 2016.

[2] Grouve, W.J.B., *Weld strength of laser-assisted tape-placed thermoplastic composites*. 2012: University of Twente.

[3] Stokes-Griffin, C. and P. Compston, *Laser-assisted tape placement of thermoplastic composites: the effect of process parameters on bond strength*, in *Sustainable Automotive Technologies 2013*. 2014, Springer. p. 133-141.

[4] Stokes-Griffin, C.M., et al., *Thermal modelling of the laser-assisted thermoplastic tape placement process.* Journal of Thermoplastic Composite Materials, 2015. 28(10): p. 1445-1462.

[5] A. Zaami, I.Baran, R. Akkerman, *Numerical Modelling of Laser Assisted Tape Winding Process.* 20th International ESAFORM-Dublin 2017, p. Under publication.

[6] Stokes-Griffin, C. and P. Compston, *A combined optical-thermal model for near-infrared laser heating of thermoplastic composites in an automated tape placement process.* Composites Part A: Applied Science and Manufacturing, 2015. **75**: p. 104-115.

[7] Abgrall, R., D.D. Santis, and M. Ricchiuto, *High-order preserving residual distribution schemes for advection-diffusion scalar problems on arbitrary grids.* SIAM Journal on Scientific Computing, 2014. **36**(3): p. A955-A983.

[8] Brunner, F., F. Frank, and P. Knabner, *FV Upwind Stabilization of FE Discretizations for Advection–Diffusion Problems*, in *Finite Volumes for Complex Applications VII-Methods and Theoretical Aspects*. 2014, Springer. p. 177-185.

[9] Halpern, L. and F. Hubert, *A finite volume Ventcell-Schwarz algorithm for advection-diffusion equations.* SIAM Journal on Numerical Analysis, 2014. **52**(3): p. 1269-1291.
[10] McLaughlin, B., J. Peterson, and M. Ye, *Stabilized reduced order models for the advection–diffusion–reaction equation using operator splitting.* Computers & Mathematics with Applications, 2016. **71**(11): p. 2407-2420.
[11] Wang, H., C.-W. Shu, and Q. Zhang, *Stability and error estimates of local discontinuous Galerkin methods with implicit-explicit time-marching for advection-diffusion problems.* SIAM Journal on Numerical Analysis, 2015. **53**(1): p. 206-227.
[12] Ismet Baran & Jesper H. Hattel & Cem C. Tutum, *Thermo-Chemical Modelling Strategies for the Pultrusion Process*, Appl Compos Mater (2013) 20:1247–1263.